ELSEVIER

Inorganica Chimica Acta 228 (1995) 243–250

Inorganica Chimica Acta

Note

A spectroelectrochemical and photochemical investigation of photoinduced electron transfer reaction between Mg(II) porphyrin and viologen

Witold S. Szulbinski [1]

Department of Chemistry, Technical University of Silesia, 44-101 Gliwice, Poland

Received 10 February 1994; revised 13 June 1994

Abstract

The spectroelectrochemical and photochemical characterization of MgTAP is presented; TAP = *meso*-tetra-*p*-(*N*-ethyl-*N*,*N*-dimethyl)anilinoporphyrin. It has been found that spectroscopic changes following one-electron oxidation of MgTAP, at $E_{1/2} = 0.78 \pm 0.01$ V versus NHE, and those succeeding photooxidation of the Mg(II) porphyrin by EtV are analogous; EtV = ethylviologen. As assigned by ESR spectroscopy, the electrochemical as well as the photochemical oxidation results in the production of the porphyrin π cation-radical, $[\mathrm{MgTAP}]^+$, as a main product. In aqueous solution of EtV, the fluorescence of MgTAP* at $\lambda_{em} = 622$ nm decreases obeying the Stern–Volmer equation ($K_{SV} = 47.7$). This suggests that the reaction proceeds by the mechanism of oxidative quenching of MgTAP* fluorescence by EtV as an electron acceptor. The reaction system consisting of MgTAP/EtV/TEA, exposed to illumination at $\lambda_{ex} = 430$ nm, results in the photogeneration of the viologen π cation-radical, $[\mathrm{EtV}]^+$, with the quantum yield of $\Phi = 0.82 \pm 0.1$ mol/einstein; TEA = triethanolamine. Application of MgTAP as an electron-donating sensitizer of water photodecomposition into hydrogen and oxygen is considered.

Keywords: Spectroelectrochemistry; Photochemistry; Photoinduced electron transfer; Magnesium; Porphyrin

1. Introduction

Many multidisciplinary research efforts have been done to prepare artificial systems that convert solar light into more useful chemical energy [1]. Recently, it has been shown that supramolecular species [2] and light-harvesting polymers and sols [3] are the most attractive systems for that purpose. However, the maximum efficiency for light conversion in all of the systems is still below that attained by green plants or photosynthetic bacteria [1]. Accordingly, extensive efforts have been made to understand the mechanistic details of the photoinduced electron transfer in synthetic and natural systems [4].

This paper discusses the application of spectroelectrochemical methods (SEC) for the study of photoinduced electron transfer reactions for a selected porphyrin system, i.e. Mg(II) *meso*-tetra-*p*-(*N*-ethyl-*N*,*N*-dimethyl)anilinoporphyrin, MgTAP, and ethyl-viologen, EtV [5]. It is shown that SEC may be used as a complementary method for the spectroscopic investigation of the reaction between the electronically excited MgTAP* and EtV. These experiments provide spectroscopic evidence that the same product of MgTAP is obtained during the electrooxidation as well as upon the photooxidation of the metalloporphyrin, under suitable conditions. The photocatalytic property of MgTAP is compared to that of ZnTMPyP [6] in terms of the quantum yield of the viologen π cation-radical photogeneration. It is demonstrated that MgTAP may be used as an electron-donating sensitizer of water photodecomposition.

2. Experimental

2.1. Materials

EtV and TEA were purchased from POCH-Gliwice and were found to be sufficiently pure for use a supplied.

---

[1] Present address: Department of Chemistry, University of Houston, Houston, TX 77204, USA.

SSDI 0020-1693(94)04173-S

MgTAP was synthesized using the method described elsewhere [7]. According to the procedure, the metalloporphyrin was obtained, directly, in water solution of the TAP ligand and 50-fold excess of $MgCl_2$ salt, under darkness, and at pH = 6.5. Purification of MgTAP was performed by recrystallization from MeOH/acetone. In an aqueous solution of 0.1 M KCl the electronic spectrum of MgTAP exhibited the following absorption bands: λ ($\epsilon \times 10^{-4}$ M^{-1} cm^{-1}) 428 (42.14); 570 (1.66); 616 (1.10) nm.

2.2. Physical techniques

UV–Vis spectra were recorded on a Beckman DU-65 or Specord UV–VIS (Carl Zeiss, Jena) spectrophotometers.

The ESR spectra were taken with a Radiopan (Poznan) spectrometer operating in the X-band.

The emission spectra were recorded on a Perkin-Elmer MPF-44A spectrofluorimeter.

The UV–Vis spectra following irradiation were obtained using a glass cell, 1×1×3 cm, equipped with a magnetic stirrer and a water jacket, at 297 K. The cell was exposed to the irradiation for 2 or 4 s, then spectra were taken in the next 5–10 s. The solution in this cell was purged with nitrogen and stirred, constantly, during intervals succeeding the spectroscopic measurements. In the experiments a 200 W halogen lamp was used as the source of irradiation, $I_0 = 1.5 \pm 0.5 \times 10^{-8}$ einstein ml^{-1} s^{-1}. The lamp was equipped with an interference filter cutting the light in the range 420–450 nm, from Carl Zeiss, Jena.

The water photolysis experiments were carried out in a cell with an arm tube, the design of which is presented elsewhere [5,8].

Electrochemical experiments were performed with a three compartment cell. The working electrode was either a 3 mm diameter glassy carbon (GC) or mini-electrode in Kel-F, (Bioanalytical Systems). The secondary electrode was a platinum wire separated by a glass frit from the working electrode compartment and the reference electrode was Ag/AgCl, in 4 M KCl (with $E_0 = 0.198$ V versus NHE), separated from the main compartment by a capillary formed by sealing a platinum wire in Pyrex. Prior to the experiments the GC electrodes were polished with 0.05 μm γ-alumina (Buehler). Residual polished material was removed from the surface by sonication in a water bath.

The electrochemical experiments were undertaken using either a computer-controlled electroanalytical system CYSY-1 (Cypress Systems, Inc.), equipped with a compact potentiostat fully integrated with an IBM-AT style personal computer, which served as the data acquisition and control interface, and/or a EG-20 (ELPAN, Lubawa) programmer and a potentiostat model EP-21, in which case the output was directly recorded on paper using a Hewlett Packard plotter type 7090A or a Goertz XY/t recorder type SE-790. Aqueous solutions typically contained 0.1 M KCl or 0.2 M acetate buffer (pH = 6.3) as supporting electrolyte.

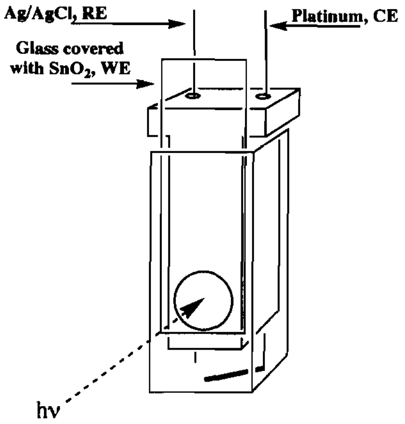

Fig. 1. Diagram showing thin-layer spectroelectrochemical cell.

ESR spectroelectrochemical experiments were done by using a thin layer cell, details of which are presented in Ref. [9]. The working electrode was made from a platinum wire.

UV–Vis spectroelectrochemical experiments (SEC) were performed by using a thin layer cell equipped with a transparent working electrode which was placed perpendicularly to the optical beam. The electrode was made from a borate glass covered with a tin oxide film (Corning Glass Co. Corning). The design of the cell is shown in Fig. 1. Further details of the spectroelectrochemical techniques may be found in Ref. [10].

3. Results

3.1. Electrochemistry

Cyclic voltammograms (CV) of MgTAP run in the potential range between 0.30 and 0.75 V versus Ag/AgCl exhibited a single set of redox peaks with the formal redox potential at $E_{1/2} = 0.575$ (0.78 ± 0.01 V versus NHE), see Fig. 2(a). The peak-to-peak separation was 75 mV and the ratio i_{cp}/i_{ap} (current of cathodic peak to current of anodic peak) was approximately 0.75 for scan speeds up to 0.25 V s^{-1}. The number of electrons (n) involved in the redox process was determined using the Malachesky equation [11] which relates n to the square of the ratio of slopes from a Randles plot (i_{cp} versus the square root of the scan rate for CV), and a Cottrell's plot (i_d versus inverse of square root of electrolysis time for chronoamperometric data). It was found that $n = 0.96 \pm 0.10$ and the diffusion coefficient, D_o, was equal to $2.1 \pm 0.8 \times 10^{-6}$ cm^2 s^{-1} for the Mg(II) porphyrin.

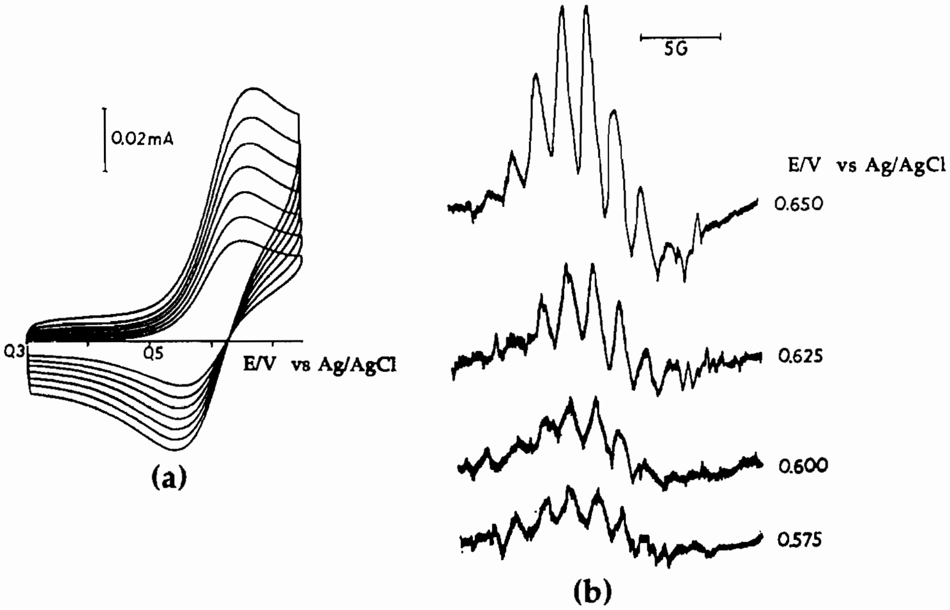

Fig. 2. (a) Cyclic voltammograms of aqueous MgTAP (1.8 mM) containing acetate buffer (0.2 M, pH = 6.4) as supporting electrolyte and run at seven scan rates: 100, 81, 64, 49, 36, 25 and 16 mV s^{-1}, respectively; (b) ESR spectra of MgTAP (2 mM) taken at $T = 24$ °C and $\nu^0 = 9.295$ GHz, and following electrooxidation at the potentials assigned on the Figure.

When the potential range was expanded, from −0.45 to 1.0 V, a further electrooxidation wave at $E_a = 0.905$ V versus Ag/AgCl occurred, see Fig. 3. The product of this reaction was reduced at $E_c = -0.11$ V versus Ag/AgCl as indicated by the CV curve of the reverse scan with switching potential at 1.0 V. The height of the cathodic peak developed at E_c depended on the scan rate and increased with the time of electrolysis at $E = 1.0$ V. Moreover, the electrooxidation at E_a was accompanied by a decay of the cathodic peak of the redox couple at $E_{1/2}$. This behavior as well as the large peak-to-peak separation, $\Delta E = 1.05$ V, indicated that the total amount of the product obtained at the second step of the electrooxidation was consumed in the follow-up hydrolysis. Approximately, equal areas under these anodic waves showed that both steps of this electrooxidation involved two electrons.

To further understand the electrooxidation of MgTAP, spectroelectrochemical measurements were undertaken. As can be seen in Fig. 3(a) and (b), distinct spectroscopic changes were observed during the first and second steps of this process, indicating that a different form of MgTAP was produced at $E_{1/2}$ than that at E_a. In the potential range of this redox couple a decrease of absorbance bands at 428 and 570 nm of the metalloporphyrin was observed. These spectroscopic changes were concomitant with the development of a new peak at 415 nm and a broad absorbance between 600 and 700 nm, respectively. When the working electrode was held at a potential large enough for the second step of electrooxidation to occur, the absorption peak at 415 nm disappeared and a new band grew at 440 nm. It is of interest that the band at 428 nm and the absorbance at 570 nm could be regenerated by stepping the potential to −0.11 V after either the first or the second step of the electrooxidation. This behavior was consistent with results of multiple CV scans which showed that the product obtained at $E_a = 0.905$ V could be transformed into MgTAP upon electroreduction at −0.11 V.

To assign a structure to the product obtained upon the first step of electrooxidation, in situ ESR spectroelectrochemical measurements of MgTAP were done. In the potential range between 0.55 and 0.65 V, see Fig. 2(b), these experiments showed a strong ESR line at $g = 2.0023$ typical of organic radicals. When the potential of the working electrode was adjusted to a value more positive than 0.65 V, the resonance disappeared. This result suggested that the ESR lines come from a paramagnetic species produced only at $E_{1/2}$. The multiplet pattern of this spectrum (nine lines with coupling constant of $a_N = 0.159$ mT) might be attributed to coupling of one electron to four ^{14}N nuclei ($I = 1$) of this porphyrin ring. It is worth noting that the spectrum resembles that of other porphyrin π cation-radicals, such as MgTPP and ZnTPP [12]. Of course, the unpaired electron could be obtained by the electrochemical removal of one electron from the porphyrin a_{1u} orbital. The ESR data are consistent with the electrochemical results presented above and support the one-electron oxidation of MgTAP at $E_{1/2}$ to the $[MgTAP]^+$ π cation-radical.

3.2. Photochemistry

To perform the spectroscopic examination of the reaction between the electronically excited MgTAP*

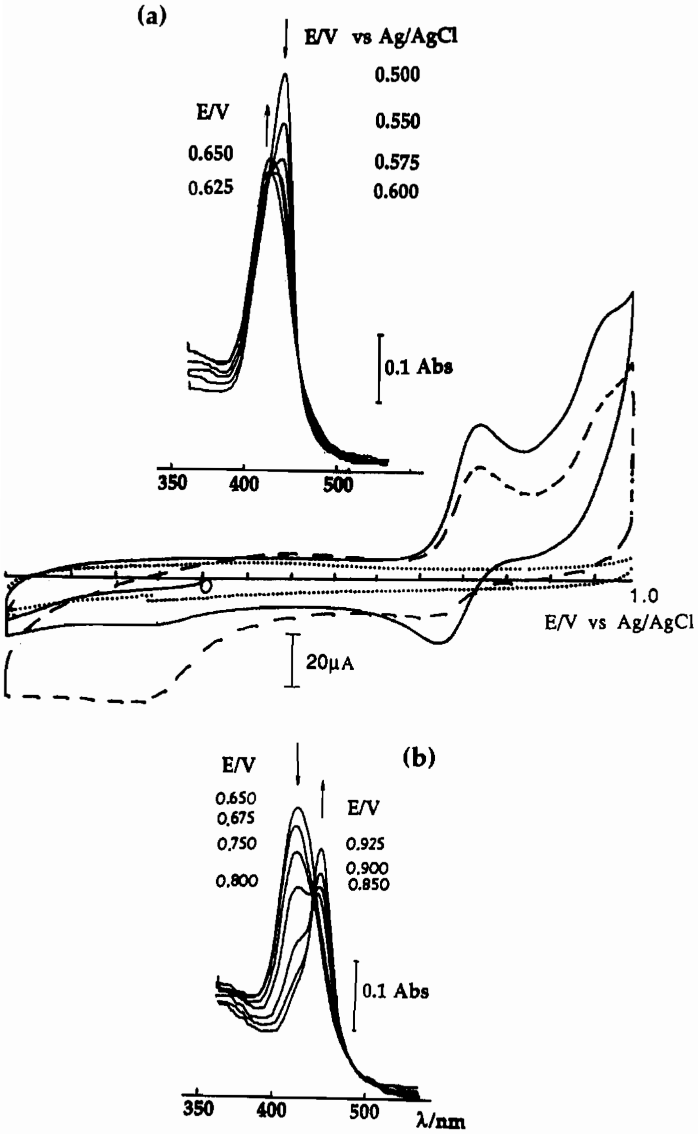

Fig. 3. CV curve (···) of aqueous acetate buffer (0.2 M, pH = 6.4); CV (——) of the same buffer but containing MgTAP, 1.8 mM; CV (– – –) of the same solution but after one-minute electrolysis at 1.0 V at $\nu = 81$ mV s^{-1}, and $T = 24$ °C. (a) and (b) UV–Vis spectra following electrooxidation of MgTAP (0.5 mM) in aqueous acetate buffer (0.2 M, pH = 6.4) taken at the first and the second step of this process, respectively.

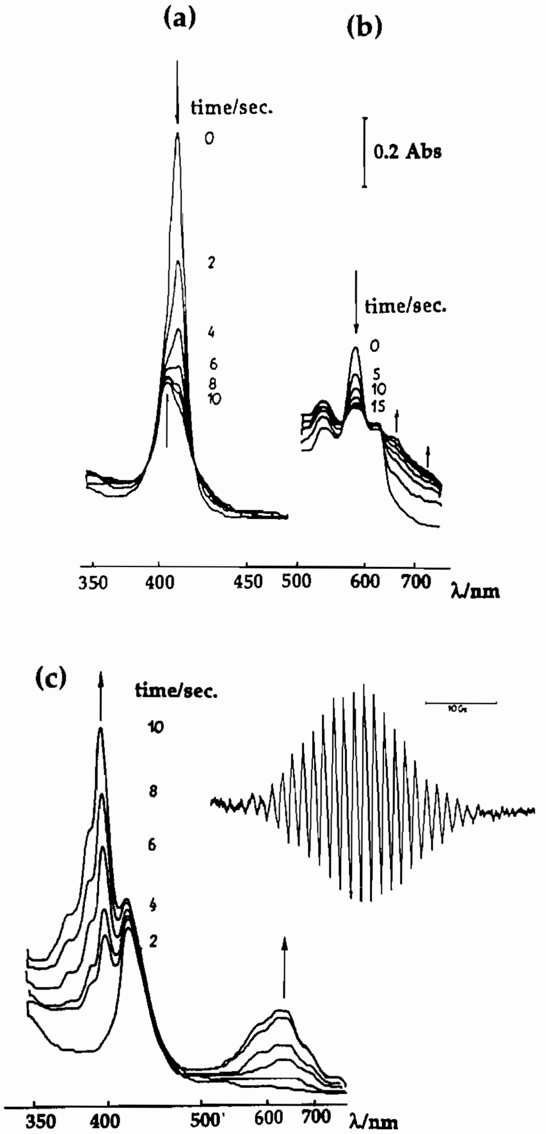

Fig. 4. UV–Vis spectra following irradiation ($\lambda_{ex} = 430$ nm; $I_0 = 1.5 \times 10^{-8}$ einstein s^{-1} ml^{-1}; $T = 24$ °C) for aqueous acetate buffer (0.2 M, pH = 6.4) containing MgTAP (2.5 μM); EtV (0.6 mM) run at the following range of wavelength ranges: (a) 350–500 nm; (b) 500–800 nm; (c) as (a) but after an addition of TEA (0.1 M). The insert shows the ESR spectrum of the same solution as (c) but after irradiation of 1 min, $\nu^0 = 9.295$ GHz.

and EtV, an aqueous solution containing equimolar amounts of the reactants (with ionic strength of 0.2 M acetate buffer, pH = 6.4) was subjected to irradiation at $\lambda_{ex} = 420 \pm 30$ nm. This wavelength was close to that of the maximum of electronic excitation of MgTAP. Following the irradiation, spectra of the solution were taken every 2 s. As can be seen from the spectroscopic changes given in Fig. 4(a) and (b), the reaction was very quick and reached completion within 10 s. These measurements showed the decay of absorbance at $\lambda_{max} = 428$ nm and the development of a band at 415 nm. Moreover, a decrease of the peak at $\lambda_{max} = 570$ nm concomitant with the increase of absorbance below 600 nm was observed. Since no more spectroscopic changes were observed within the subsequent three minutes, the final spectrum was expected to be that arising from the product. As the EtV viologen exhibits a strong oxidation property, $E_{1/2} = -0.44$ V versus NHE [13], the spectroscopic response could be ascribed to the photooxidation of MgTAP. Moreover, these spectroscopic changes were almost identical to those observed during the electrooxidation of MgTAP at $E_{1/2}$. This supports the suggestion that the [MgTAP]$^+$ π cation-radical is produced upon photooxidation of MgTAP as well as during electrooxidation of the metalloporphyrin.

In the next step, TEA was added to the reaction mixture as the sacrificial electron donor. The concentration of TEA was approximately three orders of magnitude higher than that of MgTAP and 50-fold higher than that of EtV. Immediately after the addition, new absorption bands grew at 398 and 605 nm, see Fig. 4. Over the first minute of irradiation, the absorbance increase at $\lambda_{max} = 605$ nm was linear with time, but after 15 min the curve reached a plateau which corresponded to the steady-state concentration of $[EtV]^+$, ~0.1 mM. The UV–Vis and ESR spectra presented in Fig. 4(c) apparently indicate that the viologen π cation-radical, $[EtV]^+$, was produced under these conditions [13].

In order to calculate the quantum yield of this process, Φ, the photogeneration of $[EtV]^+$ radicals by $Ru(bpy)_3^{2+}$ as the standard was performed under the same conditions as those for MgTAP (for this Ru(II) complex the Φ yield has been measured to be 0.30 mol/einstein [1c,6]). Then, these results for the standard and MgTAP, respectively, were compared using the following expression developed by Demas and Crosby [14].

$$\Phi_x = \Phi_r(A_r/A_x)(I_r/I_x)(R_x/R_r)$$

where Φ is the quantum yield, A is absorbance of the sensitizer at λ_{ex}, I is the light intensity, R is the rate of $[EtV]^+$ radical production, for the reference and unknown, respectively. The obtained value of Φ as well as others physicochemical parameters for both sensitizers are summarized in Table 1, including those for the ZnTMPyP porphyrin studied by Harriman et al. [15d,e].

Table 1
Photophysical properties of MgTAP, $Ru(bpy)_3^{2+}$ and ZnTMPyP (photoredox potential, E^*; lifetime in excited-state, τ) and the quantum yield of the generation of viologen π cation-radicals, Φ, in the reaction system containing sensitizer (0.06 mM); EtV (10 mM) and TEA (0.1 M), in aqueous acetate buffer (0.2 M, pH 6.4), at 297 K

Sensitizer	E^* (V vs. NHE)	τ (ns)	Φ (mol/einstein)
MgTAP[a]	-1.21 ± 0.01	43 ± 20	0.82 ± 0.1
$Ru(bpy)_3^{2+}$[b,c]	(-0.84)	(602)	(0.30)[d]
ZnTMPyP[e]	-0.80[f]; (-0.44)	1.4; (655×10^3)	(0.75)

[a] $\lambda_{ex} = 430$ nm.
[b] $\lambda_{ex} = 450$ nm.
[c] Ref. [15b,c].
[d] Refs. [1c,15d].
[e] Ref. [15d,e].
[f] Assuming that $E_{1/2} = 1.18$ V vs. NHE [19a,b] and $E_s = 195$ kJ mol^{-1} [15e].
Values in parentheses refer to the triplet excited state of sensitizer.

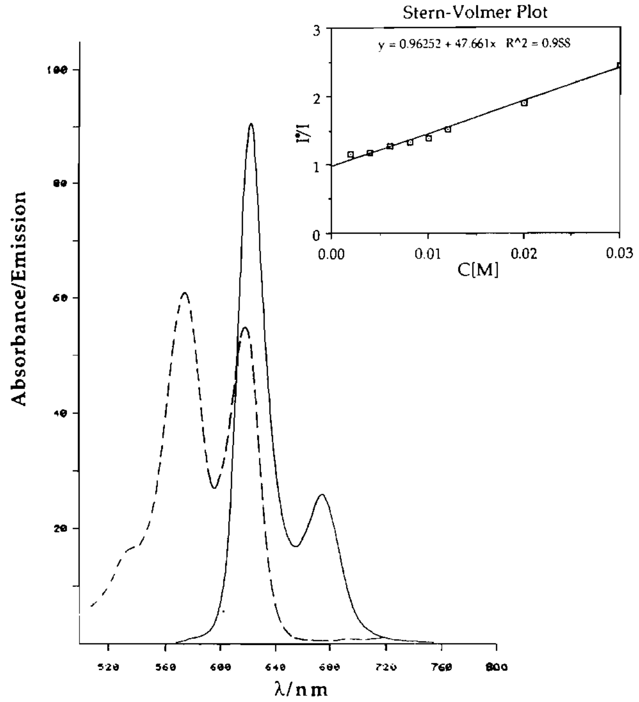

Fig. 5. Absorption and emission spectrum of aqueous MgTAP (6 μM). The insert shows a Stern–Volmer graph ($I_0/I = 1 + K_{SV}[EtV]$) [16] plotted for the quenching of MgTAP* by EtV at $\lambda_{em} = 622$ nm. Excitation line $\lambda_{ex} = 430$ nm, $T = 24$ °C.

To gain better insight into the reactivity of MgTAP*, emission spectra of the metalloporphyrin were taken in a solution of EtV. As shown in Fig. 5, the absorption and emission spectrum of aqueous MgTAP exhibited a very small Stokes shift, $\Delta\lambda = 6$ nm (distance between the Q(0,0) absorption band and the (0-0) emission band). This apparently indicates that the latter originated from the fluorescence of MgTAP. The emission spectrum exhibited two vibrational levels of the electronic transition within the porphyrin ring, the (0-0) band at $\lambda_{em} = 622$ nm and the (0-1) band at $\lambda_{em} = 678$ nm. To determine the quantum yield of the fluorescence, $\Phi_f = 0.18$, the method developed by Demas and Crosby [14] was used. It is worth noting that the Φ_f yield was approximately one order of magnitude larger than that for ZnTMPyP, $\Phi_f = 0.025$ [15d]. This suggests that the lifetime of the MgTAP singlet excited state is markedly longer than that of ZnTMPyP. Moreover, it was found that the intensity of the MgTAP fluorescence strongly depended upon the viologen concentration (at $[EtV] > 1$ mM) according to the Stern–Volmer relationship [16], see the insert of Fig. 5. This behavior shows that the reaction between MgTAP* and EtV proceeded by the mechanism of oxidative quenching of the MgTAP* fluorescence. Under these experimental conditions, no spectroscopic evidence for phosphorescence was obtained due to the strong non-radiative decay of the MgTAP* triplet excited state.

Assuming that kinetics of the quenching reaction were limited by diffusion, the singlet lifetime of MgTAP*, τ_s, was estimated from the slope of the graph presented in Fig. 5. The rate of MgTAP diffusion was calculated from the Debye expression [17], based on the size of the porphyrin ring, the MgTAP diffusion coefficient, D_o, the temperature and the solvent property, $k_d = 1.1 \times 10^9$ M^{-1} s^{-1}. Accordingly, τ_s was estimated to be 43±30 ns by substitution of the k_d rate constant for k_q in the Stern–Volmer constant equation, ($K_{SV} = k_q \tau_s$). This value is close to that of $\tau_s = 58$ ns, assigned for MgTPP by Seybold and Gouterman [18].

The photoredox potential for thc following redox couple MgTAP*/[MgTAP]$^+$, E^*, was calculated from the MgTAP redox potential $E_{1/2}$ and the singlet energy, E_s, of this porphyrin [15e,16]. In this method, the influence of the electrostatic interaction between the reactants and products, respectively, on the E^* potential is neglected. Consequently, the E_s energy of 1.99 eV obtained from the maximum of emission at the (0-0) band and the $E_{1/2}$ potential were combined according to the following expression, $E^* = E_{1/2} - E_s = -1.21 \pm 0.01$ V versus NHE.

4. Discussion

The electrochemical properties of MgTAP resemble those of other Mg(II) porphyrins soluble in water, such as MgTMPyP and MgTSPP [19b]. In comparison to MgTMPyP, the redox potential of MgTAP is negatively shifted by 0.14 V as the electron density on the TAP porphyrin ring is greater than that on TMPyP due to the inductive effect of the four *meso*-aniline substituents. Moreover, this electronic effect makes the [MgTAP]$^+$ π cation-radical more resistant in the following disproportionation [19b]. Consequently, the first step of MgTAP electrooxidation appears to be reversible over the timescale of the CV measurements. On the contrary, the two-electron oxidation product, the electrophilic [MgTAP]$^{2+}$ π dication, undergoes rapid hydrolysis into either isoporphyrin or dihydroxyporphyrin. These follow-up reactions shift the cathodic peak of the second redox couple of MgTAP to −0.11 V that, presumably, corresponds to the electroreduction of the hydroxyporphyrin derivatives.

As assigned by spectroelectrochemical measurements for UV–Vis and ESR spectroscopy, the [MgTAP]$^+$ π cation-radical is produced upon photooxidation of MgTAP by EtV, at $\lambda_{ex} = 430$ nm. In other words, the spectroscopic changes following the photooxidation of MgTAP are identical to those occurring on electrooxidation of this porphyrin at $E_{1/2}$. The [MgTAP]$^+$ radical exhibits the absorbance at $\lambda_{max} = 415$ nm and the broad electronic band over the λ range 600–700 nm, and the ESR resonance at $g = 2.0023$ with the hyperfine splitting is typical of porphyrin π cation-radicals. The spectroscopic data resemble those reported earlier for π-cation radicals derived from ZnTSPP and MgTPP [12,19].

The singlet excited state photoredox potential of MgTAP, $E^* = -1.21$ V versus NHE, implies that the metalloporphyrin upon irradiation at the maximum of excitation exhibits a strong reducing property. This is demonstrated by the photoreduction of EtV by the metalloporphyrin as the electron-donating sensitizer. In the presence of a sacrificial electron donor, such as TEA, this process shows photocatalysis. In other words, MgTAP after photooxidation by EtV is immediately reduced by TEA to this porphyrin neutral form. Thus, the photooxidation of MgTAP can happen again. The UV–Vis and ESR measurements reveal that the main product of this process is the [MgTAP]$^+$ π cation-radical, even if the TEA is dominated in the reaction mixture. These data strongly suggest that the following reduction of the [MgTAP]$^+$ radical to the MgTAP neutral form is either driven or accelerated by light. From the redox potential of MgTAP and the oxidation potential of TEA ($E_{ox} = 0.82$ V versus NHE) [15b], it is apparent that the reduction of the [MgTAP]$^+$ ground state by TEA is not allowed thermodynamically. However, upon irradiation close to the maximum of excitation ($\lambda_{max} = 415$ nm) the [MgTAP]$^+$ radical appears to be a more powerful oxidant as its oxidation potential is positively shifted by the energy of the excited state [15, 16]. Consequently, the full catalytic cycle demands two photons, the first for the excitation of MgTAP to reduce EtV, and the second for the excitation of the [MgTAP]$^+$ radical to regenerate the sensitizer by TEA, see Scheme 1.

It is known [1,21] that the generation of viologen π cation-radicals in the solution of a redox catalyst, such as colloidal Pt, leads to the reduction of water into hydrogen (the redox potential of EtV is higher than that of hydrogen on Pt, $E = -0.059$ pH V, at 297 K). Therefore, the reaction system MgTAP/EtV/TEA/Pt may be utilized for the photodecomposition of water. This process is shown schematically in Fig. 6. In this approach MgTAP functions as the sensitizer and the viologen as the electron carrier between the MgTAP and Pt particles. Up to now, several others systems incorporating Zn [20a], Sn [8,20b], Pd [20c] and

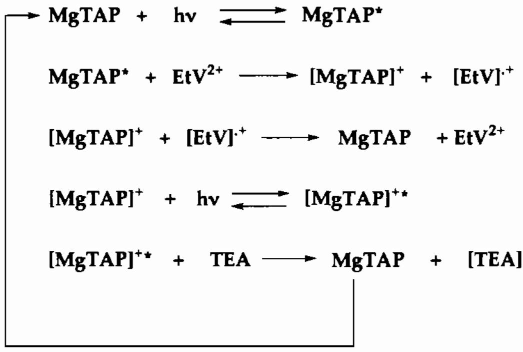

$$\mathrm{MgTAP} + h\nu \rightleftharpoons \mathrm{MgTAP}^*$$

$$\mathrm{MgTAP}^* + \mathrm{EtV}^{2+} \longrightarrow [\mathrm{MgTAP}]^+ + [\mathrm{EtV}]^{\cdot +}$$

$$[\mathrm{MgTAP}]^+ + [\mathrm{EtV}]^{\cdot +} \longrightarrow \mathrm{MgTAP} + \mathrm{EtV}^{2+}$$

$$[\mathrm{MgTAP}]^+ + h\nu \rightleftharpoons [\mathrm{MgTAP}]^{+*}$$

$$[\mathrm{MgTAP}]^{+*} + \mathrm{TEA} \longrightarrow \mathrm{MgTAP} + [\mathrm{TEA}]^+$$

Scheme 1.

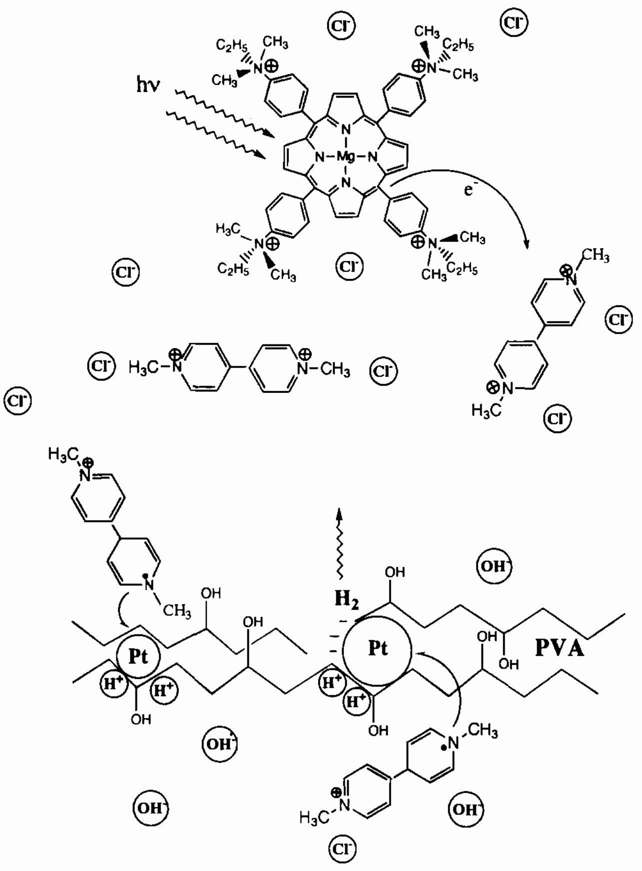

Fig. 6. Illustration of the hypothetical photoreduction of water into hydrogen using MgTAP as sensitizer, methyl-viologen as electron carrier and Pt/PVA as redox catalyst; PVA = polyvinyl alcohol.

Ru [8,15a,b,c] porphyrins or a polypyridine complex for the conversion of light into a more useful chemical energy have been suggested.

The UV–Vis examination of EtV reduction by the electronically excited state of MgTAP*, in the presence of TEA and the platinum sol, does not show any spectroscopic changes due to the viologen π cation-radical, instead of the evidence for the [MgTAP]$^+$ cation production. However, small bubbles of gas, presumably hydrogen, can be seen in the reaction mixture upon irradiation. As discussed above, this behavior may support the fact that the viologen radical is immediately consumed in the following reduction of water and the steady-state concentration of the [EtV]$^+$ radical is below that of the limit of this spectroscopic detection. In other words, the average rate of charge transfer between the Pt particles and the [EtV]$^+$ radicals, and the follow-up reduction of water on 'the polarized Pt microcathodes' is faster than that of the photogeneration and the subsequent separation of the [EtV]$^+$ radical from the [MgTAP]$^+$/[EtV]$^+$ ion-pair.

From the data presented in Table 1, it can be seen that MgTAP is a more efficient sensitizer than the others. This seems surprising, as the probability of the photoinduced electron transfer reaction should be smallest for MgTAP, in terms of the length of the lifetime τ_s. This discrepancy might be clarified based on the solvent cage-escape yield, Φ_s, of the ion-pair obtained upon the primary photoredox reaction. Of course, a comparison of the kinetics of reaction systems involving molecules with different properties and structures, such as the $Ru(bpy)_3^{2+}$ complex and MgTAP, is very difficult and must be carefully presented. Recently, it has been shown, in terms of the electrostatic forces between the positively charged reactants, that the Φ_s yield of the charge separation for the [ZnTMPyP]$^+$-[MeV]$^+$ ion-pair ($\Phi_s = 0.83$) [15e] is higher than that for the $Ru(bpy)_3^{3+}$-[MeV]$^+$ ion-pair ($\Phi_s = 0.15$) [16a,c]. Therefore, the difference in the Φ quantum yield for the generation of the viologen radicals by $Ru(bpy)_3^{2+}$ and MgTAP, may be attributed to the electrostatic interaction and the solvent cage-escape effect, respectively. However, others quantities, such as photoredox potentials, diffusion of reactance, lifetime of the excited state and mechanism of the electron transfer must also be taken into account, but this exceeds the topic of this work.

More accurate seems to be a comparison of the reactivity of MgTAP with that of ZnTMPyP. These molecules involve positively charged ligating ions (tetracation porphyrin) suggesting that the cage-escape yield is similar for both of them and the charge separation effect may be neglected in the consideration. In contrast, the photophysical properties of the porphyrins, such as the E^* potential and the τ lifetime are quite different. Furthermore, as assigned above by the emission spectroscopy measurements, the MgTAP singlet excited-state is efficiently quenched by EtV, while for ZnTMPyP, this reaction does not occur even in a large excess of the viologen (50 mM) [15d,e]. Recently, it has been argued [15e] that the quenching of ZnTMPyP* by MeV involves only the triplet excited state, the lifetime of which is markedly longer than that of the singlet state, see Table 1. In addition, the photoredox potential of ZnTMPyP shows that, thermodynamically, the quenching reaction is not allowed. However, this reaction takes place at a very slow rate as the probability of the electron transfer has been calculated to be ~0.002 [15e].

In the context of this consideration, it is interesting that the Φ quantum yield for the generation of [EtV]$^+$ radicals by MgTAP and ZnTMPyP, respectively, are similar. Presumably, the high photoredox potential of MgTAP significantly accelerates this reaction and enables the photoinduced electron transfer reaction in spite of the fact that the lifetime of the singlet excited state of MgTAP is relatively short. On the other hand, for ZnTMPyP, this reaction takes place mainly due to the long lifetime of the triplet excited-state even though the E^* potential of ZnTMPyP is small.

Accordingly, the Φ quantum yield for both of the metalloporphyrins suggests that neither the E^* photoredox potential nor the τ lifetime of the excited state controls the overall efficiency of this process but another property, such as Φ_s, may dominate. However, this conclusion needs more experimental support.

5. Conclusions

This paper reports the application of spectroelectrochemical methods for the mechanistic consideration of spectroscopic changes following photochemical reaction in the selected porphyrin system, MgTAP/EtV. This approach is significant in determining whether energy or electron transfer is involved in the process. It is shown that the complex spectroscopic changes succeeding the photoinduced electron transfer reaction are successfully simulated spectroelectrochemically. On the basis of the electrochemical and the range of spectroscopic (electronic, ESR and emission) measurements, it is argued that the reaction proceeds by the mechanism of oxidative quenching of the MgTAP* fluorescence.

Acknowledgements

Acknowledgment is made to the Polish Academy of Science and the Technical University of Warsaw for funding of this work. I also thank Professor J.W. Strojek for his invaluable help in the project.

References

[1] (a) J.S. Connolly (ed.), *Photochemical Conversion and Storage of Solar Energy,* Academic Press, New York, 1981; (b) V. Balzani and F. Scandola, in M. Grätzel (ed.), *Energy Resources Through Photochemistry and Catalysis,* Academic Press, New York, 1983, pp. 1–48; (c) K. Kalyanasundaram and M. Grätzel, *Coord. Chem. Rev., 69* (1986) 57; (d) J. Sykora and J. Sima, *Coord. Chem. Rev., 107* (1990) 153.

[2] (a) G. Denti, S. Campagna, S. Serroni, M. Ciano and V. Balzani, *J. Am. Chem. Soc., 114* (1992) 2944; (b) M.R. Wasielewski, *Chem. Rev., 92* (1992) 435; (c) A. Harriman, V. Hetiz, M. Ebersole and H. Willigen, *J. Phys. Chem., 98* (1994) 4982; (d) J. Hirota, T. Takeno and I. Okura, *J. Photochem. Photobiol. A: Chem., 77* (1994) 29.

[3] (a) N. Vlachopoulos, P. Liska, J. Augustynski and M. Grätzel, *J. Am. Chem. Soc., 110* (1988) 1216; (b) S.E. Webber, *Chem. Rev., 90* (1990) 1469; (c) A. Kay and M. Grätzel, *J. Phys. Chem., 97* (1993) 6272.

[4] (a) M.A. Fox and M. Chanon (eds.), *Photoinduced Electron Transfer,* Elsevier, Amsterdam, 1989; (b) J. Mattay (ed.), Photoinduced Electron Transfer, Vol. 156, Springer, Berlin, 1990; (c) G.A. Palmer (ed.), *Structure and Bonding,* Vol. 75, Springer, Berlin, 1991; (d) A.A. Slama-Schwok, M. Ottolenghi and D. Avnir, *Nature (London), 355* (1992) 240; K.L. Kott, D.A. Higgins, R.J. McMahon and R.M. Corn, *J. Am. Chem. Soc., 115* (1993) 5342.

[5] W.S. Szulbinski, *Ph.D. Dissertation,* Technical University of Silesia, Gliwice, Poland, 1990.

[6] K. Kalyanasundaram and M. Grätzel, *Helv. Chim. Acta, 63* (1980) 478.

[7] W. Szulbinski and M. Lapkowski, *Inorg. Chim. Acta, 123* (1986) 127.

[8] W. Szulbinski and J.W. Strojek, *Inorg. Chim. Acta, 118* (1986) 91.

[9] N. Poli, *J. Chem. Educ., 67* (1990) 970.

[10] (a) W.R. Heineman, F.M. Harkridge and H.N. Blount, in A.J. Bard (ed.), *Electroanalytical Chemistry,* Vol. 13, Marcel Dekker, New York, 1984, pp. 1–109; (b) R.L. Brike and J.R. Lombardi, in R.J. Gale (ed.), *Spectroelectrochemistry, Theory and Practice,* New York, 1988; (c) R.L. McCreery, in B.W. Rossiter and J.F. Hamilton (eds.), *Physical Methods of Chemistry,* Vol. II, Wiley, New York, 1986, p. 591.

[11] P.A. Malachesky, *Anal. Chem., 41* (1969) 1499.

[12] D. Dolphin and R.H. Felton, *Acc. Chem. Res., 7* (1974) 26.

[13] (a) L. Michaelis and W.S. Hill, *J. Gen. Physiol., 16* (1933) 859; (b) R.F. Homer and T.E. Tomilson, *J. Chem. Soc.,* (1960) 2498; (c) F. Bruin, F.W. Heineken, M. Bruin and A. Zahlan, *J. Chem. Phys., 36* (1962) 2783; (d) C.S. Johnson Jr. and H.S. Gutowsky, *J. Chem. Phys., 39* (1963) 58; (e) R.F. Anderson and R.B. Patel, *J. Chem. Soc., Faraday Trans., 80* (1984) 2693; (f) M. Lapkowski and W. Szulbinski, *Wiad. Chem. 39* (1985) 151.

[14] J.N. Demas and G.A. Grosby, *J. Phys. Chem., 75* (1971) 991.

[15] (a) T. Nash, *J. Biochem., 55* (1953) 416; (b) M. Kirch, J.-M. Lehn and J.-P. Sauvage, *Helv. Chim. Acta, 62* (1979) 1345; (c) R.J. Watts and J.N. Demas, *J. Chem. Educ., 60* (1983) 834, 803; (d) A. Harriman, G. Porter and M.-C. Richoux, *J. Chem. Soc., Faraday Trans. 2, 77* (1981) 833; (e) M.-C. Richoux and A. Harriman, *J. Chem. Soc., Faraday Trans. 1, 78* (1982) 1873.

[16] (a) N. Sutin and C. Creutz, *J. Chem. Educ., 60* (1983) 809; (b) F. Scandola and V. Balzani, *J. Chem. Educ., 60* (1983) 814; (c) C. Creutz, A.D. Keller, N. Sutin and A.P. Zipp, *J. Am. Chem. Soc., 104* (1982) 3618.

[17] P. Debye, *Trans. Electrochem. Soc., 82* (1942) 265.

[18] P.G. Seybold and M. Gouterman, *J. Mol. Spectrosc., 31* (1969) 1.

[19] (a) K.M. Kadish, *Prog. Inorg. Chem., 34* (1986) 435–605; (b) K. Kalyanasundaram and M. Neumann-Spallart, *J. Phys. Chem., 86* (1982) 5163; (c) A. Harriman, P. Neta and M.C. Richoux, *J. Phys. Chem., 90* (1986) 3444.

[20] (a) K. Kalyanasundaram and M. Grätzel, *Helv. Chim. Acta, 63* (1980) 478; (b) J.R. Darwent, P. Douglas, A. Harriman, G. Porter and M.C. Richoux, *Coord. Chem. Rev., 44* (1982) 83; (c) J.H. Fuhrhop, W. Krüger and H.H. David, *Liebigs Ann. Chem.,* (1983) 204; (d) I. Okura, S. Kusunoki and S. Aono, *Inorg. Chem., 22* (1983) 3828.